© 2017. Published by The Company of Biologists Ltd | Journal of Experimental Biology (2017) 220, 2108-2119 doi:10.1242/jeb.145706

RESEARCH ARTICLE

Mechanical adaptability of sea cucumber Cuvierian tubules involves a mutable collagenous tissue

Mélanie Demeuldre[1], Elise Hennebert[1,2], Marie Bonneel[1], Birgit Lengerer[3], Séverine Van Dyck[1], Ruddy Wattiez[4], Peter Ladurner[3] and Patrick Flammang[1,*]

ABSTRACT

Despite their soft body and slow motion, sea cucumbers present a low predation rate, reflecting the presence of efficient defence systems. For instance, members of the family Holothuriidae rely on Cuvierian tubules for their defence. These tubules are normally stored in the posterior coelomic cavity of the animal, but when the sea cucumber is threatened by a potential predator, they are expelled through the cloacal aperture, elongate, become sticky and entangle and immobilise the predator in a matter of seconds. The mechanical properties (extensibility, tensile strength, stiffness and toughness) of quiescent (i.e. in the body cavity) and elongated (i.e. after expulsion) Cuvierian tubules were investigated in the species *Holothuria forskali* using traction tests. Important mechanical differences were measured between the two types of tubules, reflecting adaptability to their operating mode: to ease elongation, quiescent tubules present a low resistance to extension, while elongated tubules present a high toughness to resist tractions generated by the predator. We demonstrate that a mutable collagenous tissue (MCT) is involved in the functioning of these organs: (1) some mechanical properties of Cuvierian tubules are modified by incubation in a cell-disrupting solution; (2) the connective tissue layer encloses juxtaligamental-like cells, a cell type present in all MCTs; and (3) tensilin, a MCT stiffening protein, was localised inside these cells. Cuvierian tubules thus appear to enclose a new type of MCT which shows irreversible stiffening.

KEY WORDS: Defence system, Mechanical properties, Ultrastructure, *Holothuria forskali*, Tensilin, Connective tissue, Echinodermata, Holothuroidea

INTRODUCTION

Some species of sea cucumbers, all belonging to the family Holothuriidae, possess peculiar defence organs, the so-called Cuvierian tubules (Hamel and Mercier, 2000; Becker and Flammang, 2010). In the genera *Holothuria*, *Bohadschia* and *Personothuria*, quiescent Cuvierian tubules are white caeca floating freely in the posterior coelomic cavity and attached in clusters at the basis of the left respiratory tree (Becker and Flammang, 2010). When an animal is threatened (e.g. by a predator), it directs its posterior end towards the stimulating source and contracts its body, resulting in the creation of a tear in the cloacal wall. The free ends of a few tubules pass through this tear and are expelled through the cloacal orifice (anus). Concomitantly, water from the respiratory tree is forcefully injected into the tubule lumen, resulting in a considerable elongation of the tubules in seawater. Elongated tubules become sticky upon contact with any surface in a matter of seconds, hence their classification in the instantaneous type of adhesion (Flammang et al., 2005; Demeuldre et al., 2014). Finally, Cuvierian tubules are autotomised at their attachment point on the left respiratory tree and are left behind. An imprudent predator will therefore be entangled in a dense network of sticky tubules while the sea cucumber is able to crawl away from the threat (VandenSpiegel and Jangoux, 1987; Flammang et al., 2002).

The remarkable efficiency of Cuvierian tubules is certainly due to their material properties, and in particular to the combination of the adhesiveness of their outer epithelium and the mechanical properties of their inner collagenous core (Flammang et al., 2002). Most of the information available on the mechanical properties of Cuvierian tubules comes from studies performed on the European species *Holothuria forskali* (Zahn et al., 1973; Bailey et al., 1982; Flammang et al., 2002), with only a few data available on the adhesion strength of other species (Flammang et al., 2002; Peng et al., 2011). The mean normal tenacity (force of adhesion per unit area) measured on glass for the Cuvierian tubules of *H. forskali* was 30 kPa (Flammang et al., 2002). A previous study (Zahn et al., 1973) also evaluated the adhesive strength of Cuvierian tubules at about 2.7×10^5 dynes cm^{-2} (27 kPa). These values fall within the range of adhesive strengths described for marine organisms using non-permanent adhesion, although they are among the lowest ones (Flammang et al., 2002, 2016). Cuvierian tubules adhere more strongly to polar (glass or steel) than to non-polar substrata (paraffin wax, polyethylene or polystyrene), indicating the importance of polar interactions in adhesion. Tubule tenacity is also influenced by factors like temperature and salinity. Flammang et al. (2002) also reported that adhesion strength increased with the time elapsed between expulsion and measurements, and explained this increase by an increasing rigidity of the tubule core with time after expulsion. Only two studies have been published on the biomechanical properties of the Cuvierian tubules in *H. forskali* (Zahn et al., 1973; Bailey et al., 1982), but their results are highly divergent. Zahn et al. (1973) measured a tensile strength of 6.0×10^7 dynes cm^{-2} (i.e. 6×10^6 Pa) for an extensibility of 180%; they also showed that there was a proportional relationship between the maximum force sustained by the tubule and the pulling speed, and an inversely proportional relationship between extensibility and pulling speed: a faster traction resulted in a higher force and a lower extensibility. In contrast, Bailey et al. (1982), also using traction tests, concluded that the resistance of the tubules was remarkably low, with a maximum tensile strength of 0.5×10^3 dynes cm^{-2} (i.e. 50 Pa) for a remarkable

[1]University of Mons, Research Institute for Biosciences, Biology of Marine Organisms and Biomimetics, Mons 7000, Belgium. [2]University of Mons, Research Institute for Biosciences, Laboratory of Cell Biology, Mons 7000, Belgium. [3]University of Innsbruck, Institute of Zoology and Center for Molecular Biosciences, Innsbruck 6020, Austria. [4]University of Mons, Research Institute for Biosciences, Laboratory of Proteomics and Microbiology, Mons 7000, Belgium.

*Author for correspondence (patrick.flammang@umons.ac.be)

P.F., 0000-0001-9938-1154

Received 6 July 2016; Accepted 22 March 2017

Journal of Experimental Biology

Journal of Experimental Biology (2017) 220, 2108-2119 doi:10.1242/jeb.145706

extensibility of 1400%. To date, no other study has been carried out to investigate this discrepancy.

As for mechanics, most of the knowledge on the morphology and fine structure of Cuvierian tubules comes from studies conducted on both quiescent (before expulsion) and elongated (after expulsion) tubules from the species *H. forskali* (Müller et al., 1972; VandenSpiegel and Jangoux, 1987; VandenSpiegel et al., 2000; Demeuldre et al., 2014). Quiescent tubules are composed, from inside to outside, of an inner epithelium surrounding a narrow lumen, a thick connective tissue layer containing collagen fibres organised in several helices running parallel to the tubular long axis, and a folded mesothelium which is responsible for adhesion. Elongated tubules present the same layers but their inner epithelium is dissociated and discontinuous, their connective tissue layer is thinner and shows extended collagen helices, and their mesothelium is unfolded. Many of the cell types constituting these different tissue layers are affected by the elongation process (see Becker and Flammang, 2010, for review), but no attempt has been made to correlate ultrastructural changes with modifications of the tubule mechanical properties. For instance, neurosecretory-like cells, whose processes form a network distributed between the collagen fibres (Becker and Flammang, 2010), are reminiscent of the juxtaligamental cells characteristic of echinoderm mutable collagenous tissues (MCT) (Wilkie, 1996; 2005). Such tissues can undergo rapid changes in their mechanical properties under nervous control via the release of stiffening proteins (e.g. tensilin; Tipper et al., 2003) by the juxtaligamental cells (Trotter et al., 2000; Wilkie, 1996, 2005; Mo et al., 2016).

The aim of this study was to characterise the mechanical properties of Cuvierian tubules in *H. forskali* by performing traction tests on both quiescent and elongated tubules, and correlate the results of these tests to modifications of the ultrastructure of the tubule tissue layers, mostly the connective tissue layer and to a lesser extent the inner epithelium, during elongation. Different factors known to influence mechanical properties, such as pulling speed, time elapsed after expulsion and bathing solution, were then tested to investigate whether it would be possible to reconcile our results with those of the two previous studies of Zahn et al. (1973) and Bailey et al. (1982). Finally, the expression of tensilin, a common MCT effector protein (Barbaglio et al., 2012), was also studied in Cuvierian tubules to investigate whether their connective tissue layer could be a MCT.

MATERIALS AND METHODS

Sea cucumber collection and maintenance, and preparation of Cuvierian tubules

Adult individuals of *Holothuria forskali* Delle Chiaje 1823 were collected at depths of 10–20 m by scuba diving in the area of the Observatoire Océanologique de Banyuls-sur-Mer (Pyrénées-Orientales, France). Animals were then transported to the Biology of Marine Organisms and Biomimetics laboratory (University of Mons, Belgium), where they were kept in a re-circulating aquarium (13°C, 33‰ salinity). Animals used in our experiments were maintained and treated in compliance with the guidelines specified by the Belgian Ministry of Trade and Agriculture.

To obtain elongated tubules, discharge was induced mechanically by pinching the dorsal integument of sea cucumbers. The expelled Cuvierian tubules were then collected in a large bucket of seawater where they scattered and floated freely, and the time at expulsion was noted. Quiescent tubules were collected by animal dissection after anaesthesia by incubation in seawater containing 0.1% propylene phenoxetol for 1 h at room temperature. Individual tubules were recovered by cutting them at their base.

Mechanical properties of elongated and quiescent tubules

Tensile tests were performed on both elongated and quiescent Cuvierian tubules with a digital force gauge (Mecmesin AFG, 2.5 N, Horsham, UK) fitted to a motorised test stand (Mecmesin VersaTest). The force gauge was accurate to the nearest 0.0005 N. Elongated tubules (about 40 cm in length) were mounted on the test apparatus by rolling up their two ends around the two opposite hooks, whereas quiescent tubules (about 2 cm in length) were attached with two surgical clips. Care was taken to ensure that the tubule was well attached and tight, without exerting any force on the gauge. The distance between the two hooks/clips was then recorded and corresponds to the initial length of the tubule. Although the tensile tests were conducted in air, tubules were kept in seawater or in treatment solutions until the last moment and always remained wet. All tests were completed during the first 4 h after the expulsion of tubules in seawater. Unless otherwise indicated, tensile tests were performed at a constant extension rate of 25 mm min^{-1} until failure of the tubule. Failure never occurred at the level of the clip/hook. The initial length of the tubule, together with the time required to break it at a constant extension rate, was subsequently used to calculate the final length at failure. The mechanical tests were performed and repeated with at least three individuals for each type of tubule. Data were continuously recorded as force–extension curves and these curves were then converted into stress–strain curves. True values of strain and stress were used instead of nominal values because of the high extensions (more than 10%) observed for Cuvierian tubules (Shadwick, 1992). The connective tissue cross-sectional area, measured on histological sections (see 'Morphological and ultrastructural study of quiescent and elongated Cuvierian tubules', below), was used for the calculation of the true stress instead of the tubule wall cross-sectional area because the former tissue is the most important in terms of thickness and appears clearly as the layer bearing all the load exerted on a Cuvierian tubule. Several material properties of the Cuvierian tubules, i.e. extensibility, strength, stiffness and toughness, were calculated according to the formulae of Vogel (2013). The true strain ε expresses the deformation of the Cuvierian tubule in response to a certain stress and, at the point at which the tubule fails (at final length), it is a measure of the material's extensibility. Similarly, the maximum value of true stress σ is an indicator of the tubule tensile strength. The tangent modulus of elasticity E is a measure of the tubule stiffness. For elongated tubules, this modulus was measured as the highest slope of the stress–strain curve and thus corresponds to the maximum stiffness of the tubule (E_{max}). For quiescent tubules, the initial modulus (E_{init}) or Young's modulus was used. Finally, we calculated the strain energy storage, which is the energy needed to extend and break the tubule per unit of volume (product of the initial length of the tubule and the connective tissue cross-sectional area). This is a measure of the tubule toughness.

Some conditions of the tests were modified in order to evaluate their influence on the mechanical properties of elongated and quiescent tubules. First, a pulling speed of 250 mm min^{-1} was tested on the elongated tubules. Measurements of the mechanical properties of these tubules were also realised at different times after expulsion. These times varied from a few minutes up to 4 h. Finally, in order to investigate the occurrence of a MCT, both quiescent and elongated Cuvierian tubules were incubated in seawater containing 1% Triton X-100, a non-ionic detergent that lyses cells. Control tubules were kept in natural seawater for the same length of time.

All statistical tests were performed with the software Statistica (StatSoft, Tulsa, OK, USA). For traction tests, the results were analysed in order to look for significant differences in the

Journal of Experimental Biology (2017) 220, 2108-2119 doi:10.1242/jeb.145706

mechanical properties of the Cuvierian tubules between the different bathing solutions and between the pulling speeds. Data were analysed by *t*-tests or Mann–Whitney *U*-tests. Holothuroid individuals were always used as the replicate (i.e. the mean value of the measurements performed on the different tubules of a single individual was used in the tests). Regression analysis was also used to search for significant relationships between the mechanical properties and the time after expulsion for elongated tubules. In this case, all sea cucumber individuals were pooled. The level of significance was always set at α=0.05.

Morphological and ultrastructural study of quiescent and elongated Cuvierian tubules

Quiescent and elongated Cuvierian tubules were obtained as described previously. Some tubules were fixed in Bouin's fluid for 24 h. They were subsequently dehydrated in a sequence of graded ethanol, embedded in paraffin wax using a routine method and cut transversely into 10 µm-thick sections with a Microm HM 340 E microtome (Thermo Fisher Scientific, Waltham, MA, USA). The sections were mounted on clean glass slides and stained with Heidenhain's Azan trichrome (Gabe, 1968). Other tubules were fixed for 3 h at 4°C in 3% glutaraldehyde in cacodylate buffer (0.1 mol l^{-1}, pH 7.8; adjusted to 1030 mOsm l^{-1} with NaCl). They were then rinsed in cacodylate buffer, post-fixed for 1 h in 1% OsO_4 in the same buffer, dehydrated through an ethanol series and embedded in Spurr resin. Semi-thin sections (1 µm) were cut with a Reichert Om U2 ultramicrotome (Vienna, Austria) equipped with a glass knife. The sections were then stained with a 1:1 mixture of 1% aqueous solution of Methylene Blue in 1% sodium tetraborate and 1% aqueous solution of Azur II. Ultrathin sections (40–70 nm) were cut with a Leica Ultracut UCT ultramicrotome (Wetzlar, Germany) equipped with a diamond knife. They were stained with uranyl acetate and lead citrate. Paraffin and semi-thin sections were observed with a Zeiss AxioScope A1 microscope equipped with an AxioCam ICc3 camera (Zeiss, Oberkochen, Germany). Images were acquired using the Zeiss AxioVision 4.7 software. Ultra-thin sections were observed with a Zeiss LEO 906E transmission electron microscope. Images were acquired using Zeiss AnalySIS software.

Tensilin expression and localisation in Cuvierian tubules

To date, the protein sequence of tensilin is only available for the species *Cucumaria frondosa* (Tipper et al., 2003) and *Apostichopus japonicus* (L. Li and C. He, unpublished data). These sequences were retrieved from NCBI (accession numbers AAK61535 and KR002726.1, respectively) and were used for a tBLASTn search in the Cuvierian tubule transcriptome from *H. forskali* available in our laboratory (purchased from GIGA-Genomics, Liège, Belgium). Information about transcriptome sequencing and *de novo* assembly are presented in the Appendix. Only transcripts with a bit score above 80 were considered and their FPKM (fragments per kilobase of transcript per million mapped reads) values were used to estimate their relative abundance in the Cuvierian tubule transcriptome (Haas et al., 2013). One transcript was selected to design probes to perform *in situ* hybridisation and to raise antibodies for western blots and immunohistochemistry.

For total RNA extraction, Cuvierian tubules were rapidly dissected from one sea cucumber and immediately frozen in liquid nitrogen. They were then homogenised in Tri Reagent solution (Applied Biosystems, Foster City, CA, USA) using a Silent crusher-M homogeniser (Heidolph, Schwabach, Germany), and total RNA was extracted according to Applied Biosystem's instructions. A 1 µg aliquot of total RNA was reverse transcribed using the 1st Strand cDNA Synthesis Kit for RT-PCR (AMV; Roche, Basel, Switzerland). Whole-mount *in situ* hybridisation was performed according to Lengerer et al. (2014) with the following changes: (1) template DNA for producing DIG-labelled probe (501 bp) was made using Q5 High-Fidelity DNA polymerase (New England Biolabs, Ipswich, MA, USA) with the forward primer 5′-CAGTGCTCTGATCATCGATTCTTT-3′ and reverse primer 5′-TCTCTCATTTTGAAGCAATCTTCG-3′. A T7 promoter binding site was added to the reverse strand PCR primer and a Sp6 promoter binding site was added to the forward primer for negative control; (2) the heat fixation step at 80°C was omitted; and (3) colour development was performed in NBT/BCIP plus Suppressor 1-Step Solution (Thermo Fisher Scientific). The labelled tubules were embedded in Tissue Tek O.C.T. medium (Sakura, The Netherlands) and frozen at −80°C. Cryosections of 5 µm in thickness were performed using a CM 1950 cryostat (Leica) and dried at room temperature. The sections were incubated in water for 1 min to remove excess embedding medium and were air dried again. They were observed and photographed with the Zeiss AxioScope A1 microscope.

Polyclonal antibodies were obtained by immunisation of a rabbit with a synthetic peptide (VVTGNKETDTDGSTY, chosen within the translated protein sequence of the selected transcript based on its potential for successful synthesis and immunogenicity) conjugated to keyhole limpet haemocyanin (Eurogentec, Liège, Belgium). The antibodies were isolated from the crude serum by affinity purification using the synthetic peptides (Eurogentec).

For western blot analyses, Cuvierian tubules were rapidly dissected from one sea cucumber anaesthetised in a solution of 0.1% 1-phenoy-2-propanol in seawater and immediately frozen at −80°C for a minimum of 3 h in 2 volumes of the following buffer: 20 mmol l^{-1} Tris-HCl, 2 mol l^{-1} NaCl, 10 mmol l^{-1} EGTA (pH 8.0) containing protease inhibitors. Cuvierian tubules were thawed on ice, cut into small pieces and homogenised in the buffer using a Heidolph Silent Crusher-M homogeniser. The homogenate was frozen again overnight at −80°C. After thawing on ice, the Cuvierian tubule extract was centrifuged for 30 min at 26,900 ***g*** and the supernatant was loaded on a 10% (w/v) SDS-PAGE gel. After electrophoresis, the proteins were blotted onto a PVDF membrane using 25 mmol l^{-1} Tris, 192 mmol l^{-1} glycine and 25% (v/v) methanol as transfer buffer. The membrane was washed with Tris-buffered saline (25 mmol l^{-1} Tris, 125 mmol l^{-1} NaCl, pH 8.0) containing 0.05% (v/v) Tween-20 (TBS-T) and then blocked overnight at 4°C in TBS-T with 5% (w/v) powdered milk (TBS-T-PM). The membrane was incubated for 90 min with the anti-VVTGNKETDTDGSTY antibody diluted 1:5000 in TBS-T-PM. After five washes of 5 min in TBS-T, peroxidase-conjugated goat anti-rabbit immunoglobulin (32460, Invitrogen, Carlsbad, CA, USA) diluted 1:750 in TBS-T-PM was applied on the membrane for 1 h. Finally, the membrane was washed again in TBS-T and immunoreactive bands were visualised using SuperSignal™ West Femto Maximum Sensitivity Substrate (Pierce, Waltham, MA, USA).

For immunohistochemistry, Cuvierian tubules were fixed in 4% (w/v) paraformaldehyde in phosphate-buffered saline (PBS; pH 7.4), rinsed in PBS, dehydrated through an ethanol series, embedded in paraffin and cut transversally into 4 µm-thick sections. These sections were subjected to indirect immunohistochemistry according to the following protocol. After deparaffinisation, sections were blocked for 30 min in TBS-T with 3% (w/v) bovine

Journal of Experimental Biology (2017) 220, 2108-2119 doi:10.1242/jeb.145706

serum albumin (BSA; TBS-T-BSA). They were then washed 3 times in TBS-T. The anti-VVTGNKETDTDGSTY antibody diluted 1:2000 in TBS-T-BSA was applied to the sections for 1.5 h. After three washes of 5 min in TBS-T, the sections were incubated for 30 min in anti-rabbit immunoglobin conjugated to peroxidase (ImmPRESS Reagent anti-rabbit, Vector Laboratories, Burlingame, CA, USA) and washed again in TBS-T (3×10 min). Immunoreactivity was visualised using diaminobenzidine tetrahydrochloride (DAB; Sigma-Aldrich, St Louis, MO, USA), with Luxol Blue as a counterstain. Alternatively, Alexa Fluor 594-conjugated goat anti-rabbit immunoglobulin (A-11012, Invitrogen; diluted 1:100 in TBS-T-BSA and incubated for 1 h) was used as the secondary antibody and sections were mounted with Vectashield (Vector Laboratories) and observed in epifluorescence. Control reactions were performed by replacing the primary antibody with TBS-T-BSA. Sections were observed and photographed using the Zeiss AxioScope A1 microscope.

RESULTS

Mechanical properties of quiescent and elongated Cuvierian tubules

Typical force–extension and stress–strain curves for quiescent tubules are presented in Fig. 1 and the material properties measured for traction tests performed in seawater are presented in Table 1. The two curves show a similar pattern characterised by a large plateau at low values followed by several peaks until the tubule finally breaks. The average force at the plateau is very low, i.e. 0.006±0.003 N, meaning that the tubule does not resist traction up to a considerable deformation (about 6.5 times its initial length). The maximal force reaches 0.028±0.037 N, corresponding to a tensile strength of 0.883±1.323 MPa. At this maximum stress, the strain of the tubule is 1.961±0.705. The final extensibility reaches a value of 2.009±0.723. E_{init} (Young's modulus) and toughness are 0.044±0.040 MPa and 0.108±0.129 MJ m^{-3}, respectively. E_{init} was measured instead of E_{max} because of the very irregular and unreproducible pattern of stress peaks at the end of the curve, which was presumably due to sliding of the clips along the tubule.

The force–extension and stress–strain curves for elongated Cuvierian tubules were totally different from the curves obtained for quiescent tubules, being typically bell shaped (Fig. 2). Characteristically, there was an initial region of low resistance of the tubule to the applied force, followed by a region presenting a sudden increase in stress until a yield point after which the stress decreased regularly, through successive steps. There was therefore no sudden rupture of the tubule but rather a progressive dislocation of the tissue. From these measurements, we obtained a maximal force of 0.672±0.173 N, corresponding to a tensile strength of 3.209±0.838 MPa. At maximum stress, the strain of the tubule was 0.266±0.029. Values for extensibility, E_{max} and toughness were 0.483±0.054, 19.705±3.673 MPa and 0.664±0.173 MJ m^{-3}, respectively (Table 1). We also investigated the effect of traction speed on elongated Cuvierian tubules. A pulling speed of 250 mm min^{-1} induced significant differences in nearly all the measured and calculated parameters compared with a pulling speed of 25 mm min^{-1}. Indeed, all parameters were significantly higher for the higher pulling speed, except for stiffness, for which there was no statistical difference between the two speeds (Table 2).

Comparative morphology and ultrastructure of quiescent and elongated tubules

To correlate the results of the mechanical tests with potential modifications of the Cuvierian tubule tissue layers during elongation, the morphology and ultrastructure of quiescent and elongated tubules were compared. Our observations on the morphology of the Cuvierian tubules of *H. forskali* corroborate those of Müller et al. (1972) and VandenSpiegel and Jangoux

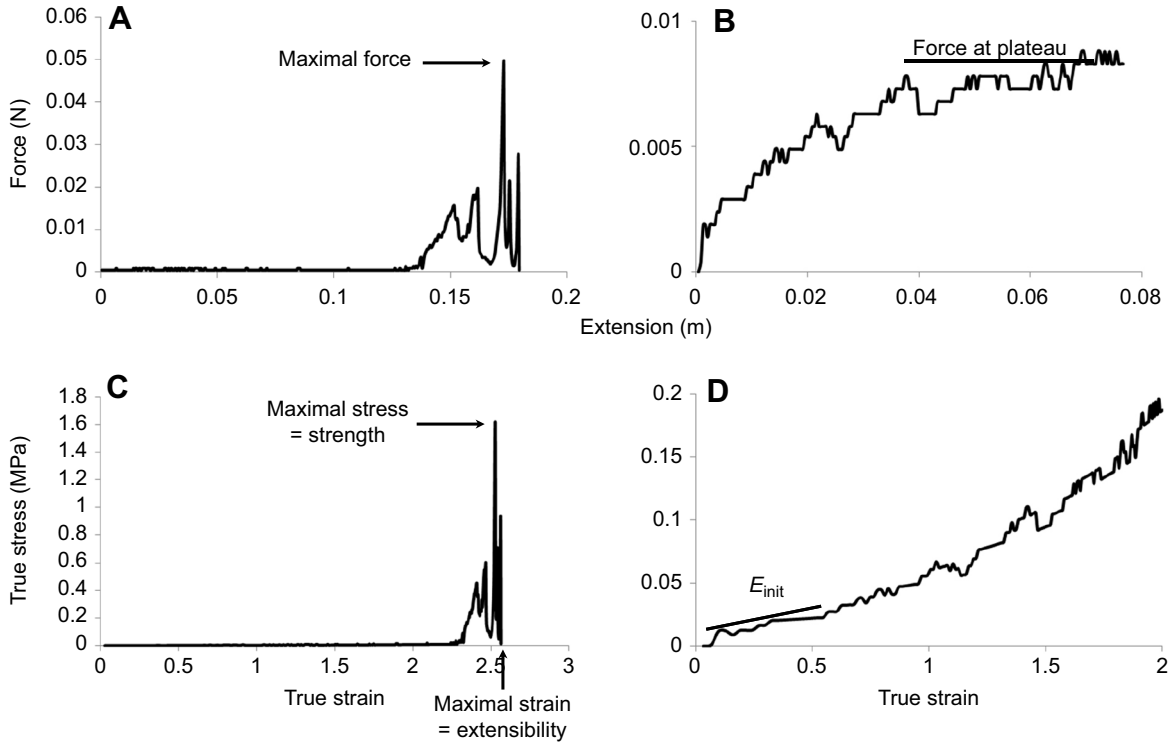

Fig. 1. Traction test on quiescent Cuvierian tubules from *Holothuria forskali*. (A,C) Typical force–extension (A) and stress–strain (C) curves, showing the material properties measured. (B,D) Expanded view of the initial part of another force–extension (B) and stress–strain (D) curve. E_{init}, initial stiffness.

Journal of Experimental Biology

Journal of Experimental Biology (2017) 220, 2108-2119 doi:10.1242/jeb.145706

Table 1. Comparison of the mechanical properties of quiescent and elongated Cuvierian tubules from *Holothuria forskali* in two bathing solutions

	Solution						
	Seawater	Triton X-100	*t*	*U*	*Z*	d.f.	*P*
Quiescent tubules							
Maximal force (N)	0.028±0.037	0.025±0.022	0.095			3	0.930
ε	1.961±0.705	8.196±8.368		1.000	−0.866	3	0.400
Extensibility	2.009±0.723	8.595±8.777		1.00	−0.866	3	0.400
Strength (MPa)	0.883±1.323	0.618±0.736	0.250			3	0.819
Toughness (MJ m^{-3})	0.108±0.129	0.897±0.837		0.000	−1.443	3	0.200
Force at plateau (N)	0.006±0.003	0.014±0.002	−3.311			4	0.030
E_{init} (MPa)	0.044±0.040	0.103±0.017	−2.372			4	0.077
Elongated tubules							
Maximal force (N)	0.672±0.173	0.790±0.033		9.000	−0.510	9	0.630
ε	0.266±0.029	0.214±0.011	3.003			9	0.015
Extensibility	0.483±0.054	0.417±0.056	1.803			9	0.105
Strength (MPa)	3.209±0.838	3.593±0.258	−0.758			9	0.468
Toughness (MJ m^{-3})	0.664±0.173	0.452±0.062		2.000	1.939	9	0.048
E_{max} (MPa)	19.705±3.673	28.311±1.784	−3.799			9	0.004

Values are means±s.d. For quiescent tubules, *n*=3 for seawater and *n*=2 for Triton X-100 (except for the force at plateau and stiffness, for which *n*=3 for both media), whereas for elongated tubules, *n*=8 for seawater and *n*=3 for Triton X-100. ε, true strain corresponding to maximal force; E_{init}, initial stiffness; E_{max}, maximum stiffness.

(1987) on the same species. The fine structure of the mesothelium and its modification following the elongation process have already been described in a previous work (Demeuldre et al., 2014), so we will focus here on the other tissue layers.

Most of the volume of quiescent tubules is occupied by a thick connective tissue layer, which forms about 90% of the thickness of the tubule cross-section (Fig. 3A). The mean connective tissue cross-sectional area was 3.85×10^{-7} m^2. In the inner sheath of the connective tissue layer, numerous neurosecretory-like cells filled with electron-dense granules were observed (Fig. 3B–E). Two different cell types were distinguished: type 1 neurosecretory-like cells containing large granules (diameter ranging between 0.3 and 0.6 µm) and type 2 neurosecretory-like cells containing small granules (diameter ranging between 0.2 and 0.4 µm). Processes from these two cell types are often observed in pairs, closely associated with one another (Fig. 3C,E). However, cell bodies have only been observed for type 1 neurosecretory-like cells. These cells have a small cell body presenting one long process insinuating itself between the collagen fibres and coming in close contact with the collagen fibrils (Fig. 3D,E). Another cell type, the so-called vacuolar cells, was identified close to the mesothelium (Fig. 3F). These oval-shaped cells measure approximately 12 µm in length and 4 µm in width. They are filled with numerous polygonal vacuoles measuring about 0.7 µm in diameter. The lumen of the quiescent Cuvierian tubule is inconspicuous and delimited by the inner epithelium, which is made up of flattened cells possessing a basal process (Fig. 3B). A final cell type, the spherulocytes (Fig. 3B, G), also belongs to the inner epithelium, with a single basal lamina lining both spherulocytes and epithelial cells. Spherulocytes are bulky cells containing enlarged spherules of various sizes ranging from 1.4 to 3.4 µm (Fig. 3G). They are always closely associated with the basal processes of the epithelial cells.

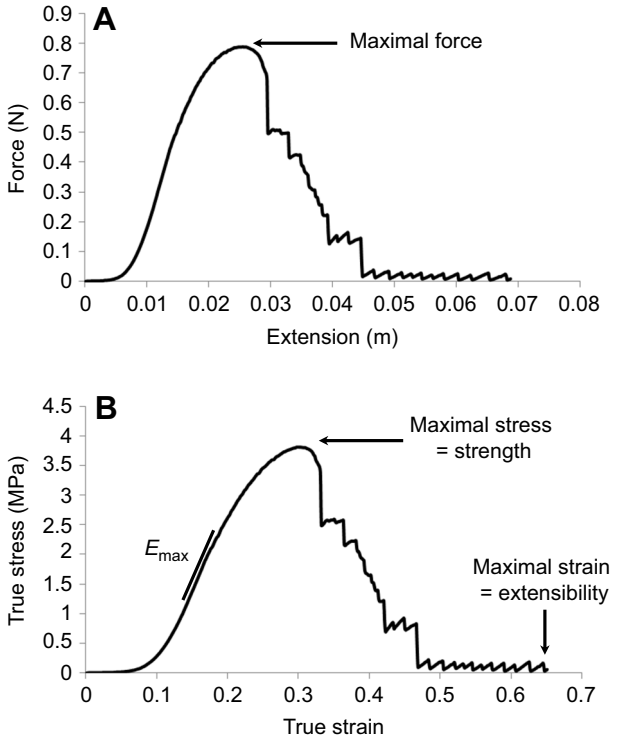

Fig. 2. Traction test on elongated Cuvierian tubules from *H. forskali*. Typical force–extension (A) and stress–strain (B) curves, showing the material properties measured. E_{max}, maximum stiffness.

During Cuvierian tubule elongation, several tissue modifications occur: the lumen diameter increases whereas the thickness of the connective tissue layer decreases because the helicoidally arranged collagen fibres stretch (Fig. 4A,B). In elongated tubules, the connective tissue layer, though still the most important layer, represents less than 50% of the thickness of the tubule cross-section (Fig. 4A) and has a mean surface area of 1.39×10^{-7} m^2. Although the connective tissue layer deformation during tubule elongation makes it difficult to estimate cell modifications in terms of both number and morphology, several changes are conspicuous. There are still a few processes from both types of neurosecretory-like cell (Fig. 4C,D). However, the cell bodies of type 1 neurosecretory like cells are no longer visible. Moreover, their cell processes always contain a much smaller number of granules (Fig. 4C,D). Vacuolar cells have also completely disappeared. The inner epithelium has become fragmented, with most epithelial cells being dislocated but with some fragments remaining attached to their basal lamina (Fig. 4B). Spherulocytes are no longer observed in elongated tubules.

Journal of Experimental Biology (2017) 220, 2108-2119 doi:10.1242/jeb.145706

Table 2. Comparison of the mechanical properties of elongated Cuvierian tubules from *H. forskali* for two pulling speeds in seawater

	Pulling speed (mm min^{-1})						
	25	250	*t*	*U*	*Z*	d.f.	*P*
Maximal force (N)	0.633±0.231	0.924±0.159	–3.023			16	0.008
ε	0.265±0.039	0.554±0.075		0.000	–3.510	16	<0.001
Extensibility	0.454±0.037	1.028±0.131		0.000	–3.510	16	<0.001
Strength (MPa)	3.337±1.106	6.301±0.996	–5.898			16	<0.001
Toughness (MJ m^{-3})	0.724±0.253	2.771±0.708		0.000	–3.510	16	<0.001
E_{max} (MPa)	20.122±6.668	15.216±1.887		19.000	1.821	16	0.068

Values are means±s.d. (n=10 for pulling speed of 25 mm min^{-1} and n=8 for pulling speed of 250 mm min^{-1}). ε, true strain corresponding to maximal force; E_{max}, maximum stiffness.

Effect of different factors on the mechanical properties of Cuvierian tubules

The remarkable similarity between the neurosecretory-like cells of Cuvierian tubules and juxtaligamental cells suggests the presence of a MCT in these organs. To further validate this hypothesis, tubule mechanical testing was repeated in seawater containing 1% Triton X-100, a cell-disrupting solution known to induce a stiffening response in different echinoderm MCTs (see Wilkie, 2002, for a review). The results are presented in Table 1. In quiescent Cuvierian tubules, the only parameter presenting a statistically significant

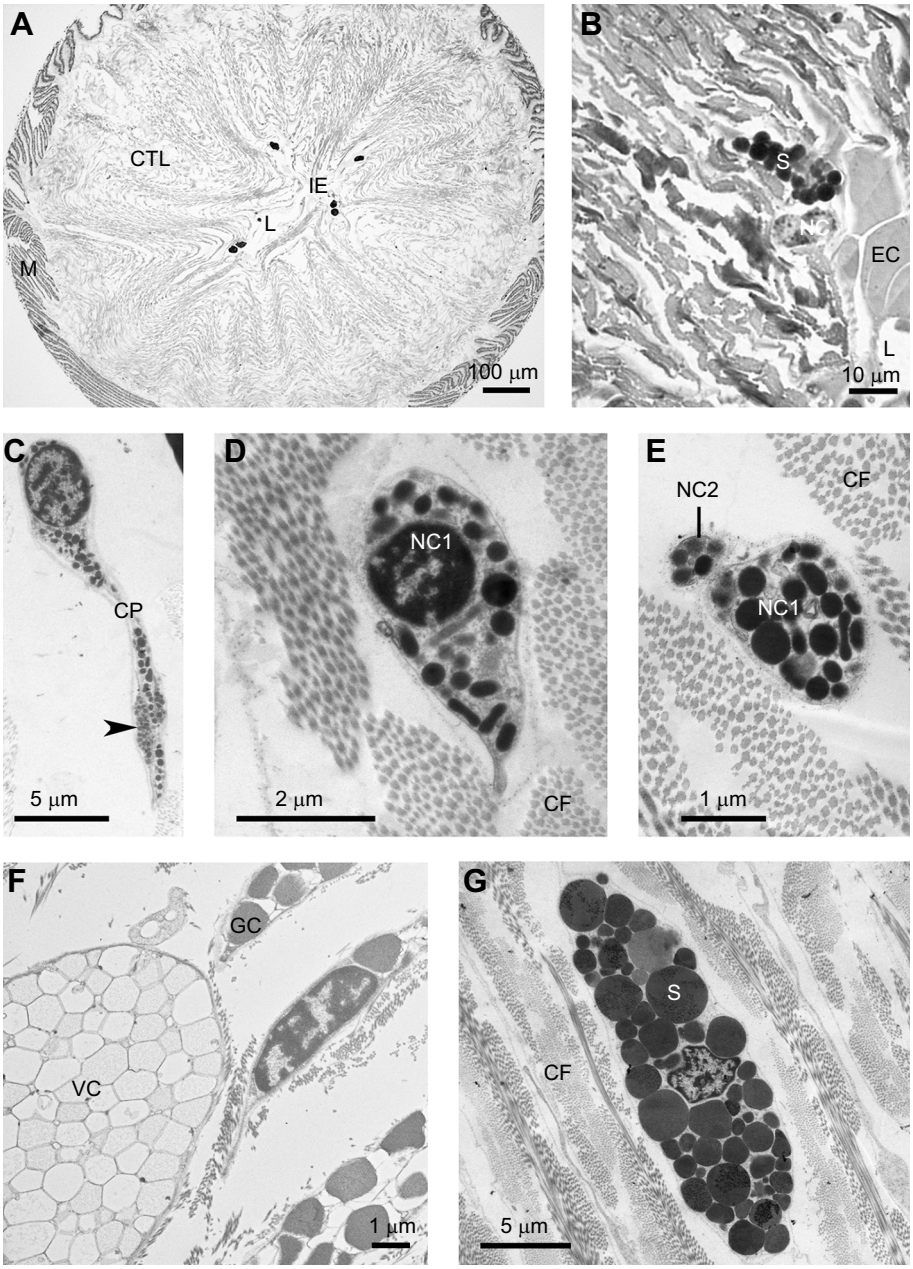

Fig. 3. Quiescent Cuvierian tubules of *H. forskali*. Cuvierian tubules were observed under light microscopy (A,B) and transmission electron microscopy (TEM; C–G). (A) Transverse section through a quiescent tubule. (B) Detail of the inner epithelium. (C) Type 1 neurosecretory-like cell with a long process (arrowhead indicates type 2 neurosecretory-like cell process). (D) Detail of a type 1 neurosecretory-like cell body. (E) Detail of cell processes from the two types of neurosecretory-like cells. (F) Vacuolar cell located near the granular cells of the mesothelium. (G) Spherulocyte located near the inner epithelium. CF, collagen fibrils; CP, cell process; CTL, connective tissue layer; EC, epithelial cell; IE, inner epithelium; GC, granular cell; L, lumen; M, mesothelium; NC, neurosecretory-like cell; NC1, type 1 neurosecretory-like cell; NC2, type 2 neurosecretory-like cell; S, spherulocyte; VC, vaculolar cell.

Journal of Experimental Biology (2017) 220, 2108-2119 doi:10.1242/jeb.145706

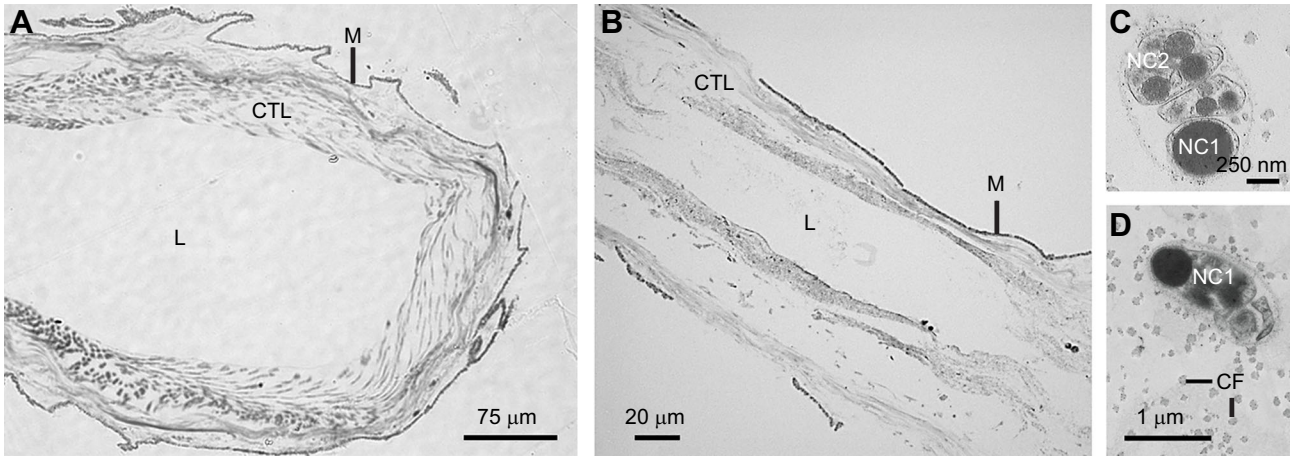

Fig. 4. Elongated Cuvierian tubules of *H. forskali*. (A,B) Transverse and longitudinal sections through elongated tubules, respectively, under light microscopy. (C,D) Processes from neurosecretory-like cells under TEM. CF, collagen fibrils; CTL, connective tissue layer; L, lumen; M, mesothelium; NC1, type 1 neurosecretory-like cell; NC2, type 2 neurosecretory-like cell.

difference between the two bathing solutions was the force at plateau (Table 1). A marginally significant difference was also noticed for Young's modulus (Table 1). Both parameters were increased when tubules were incubated in the Triton X-100 solution. The influence of the bathing medium on elongated Cuvierian tubules was also studied. The Triton X-100 solution had no influence on strength and extensibility but it decreased the true strain at maximal force and the toughness, and increased the stiffness (Table 1).

Finally, to investigate whether mechanical properties vary after Cuvierian tubule elongation, the time elapsed between tubule expulsion and traction tests was varied from 1 min up to 4 h. Values for most properties first increased to reach a maximum after 2 h and then decreased to return to the initial level (Fig. 5). This relationship between the mechanical properties and time after expulsion was best fitted by a polynomial regression (order two) for all material properties except stiffness (Table 3).

Tensilin localisation in quiescent Cuvierian tubules

To date, only one MCT stiffening protein, tensilin, has been fully characterised in echinoderms (Wilkie, 2005; Barbaglio et al., 2012). The protein sequences of tensilin from *C. frondosa* and *A. japonicus* were used to perform a tBLASTn search in the Cuvierian tubule transcriptome. Among the six transcripts whose translated sequences presented a significant homology with known tensilins (see Appendix), we selected transcript comp85694 for further investigation because it was the most abundant (in terms of FPKM) in the transcriptome and because we identified peptide sequences specific to this transcript at the proteomic level (Demeuldre, 2015; see Appendix). The protein sequence corresponding to transcript comp85694 presented 42.3% and 44.9% identity with the sequences of tensilin from *C. frondosa* and *A. japonicus*, respectively (Fig. 6). The full-length protein sequence consists of a 20 amino acid-long predicted signal peptide and a 257 amino acid-long secreted protein sequence corresponding to a calculated molecular mass of 29 kDa. The sequence of tensilin from the Cuvierian tubules of *H. forskali* has been deposited in the GenBank database under accession number KY609179.1.

In situ hybridisation was performed to localise the mRNAs coding for tensilin in Cuvierian tubules (Fig. 7). Probes were designed based on the sequence of the selected transcript. Strongly labelled cells were observed at the level of the connective tissue layer (Fig. 7A,C). Their size, shape and location between the collagen fibres indicate that they correspond to the cell bodies of neurosecretory-like cells. A weaker labelling was also detected at the level of the inner epithelium, probably around the epithelial cells (Fig. 7A). The labelling of the peritoneocytes in the mesothelium seems to be non-specific as it was also observed in the negative controls (sense probes; Fig. 7B).

To further confirm the expression and localisation of tensilin in the Cuvierian tubules, we raised polyclonal antibodies directed against one peptide (VVTGNKETDTDGSTY) selected in the translated sequence of comp85694, and used them in western blots

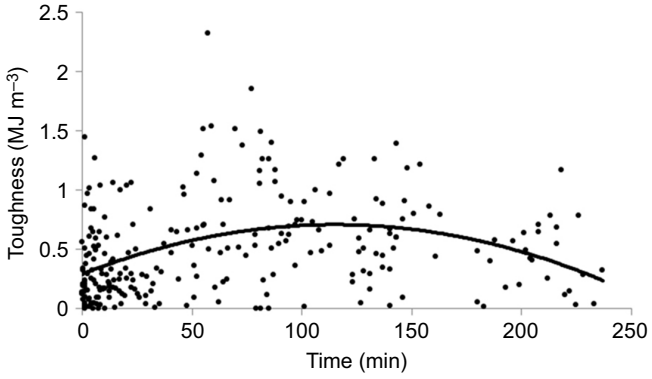

Fig. 5. Relationship between the toughness of elongated Cuvierian tubules and the time elapsed after their expulsion. n=254.

Table 3. Relationship between the mechanical properties and the time after expulsion for elongated Cuvierian tubules from *H. forskali* expelled in seawater

	Equation	R^2	P
Maximal force	y=–2.592E–5x^2+0.006x+0.306	0.15	0.001
True strain corresponding to maximal force	y=–6.510E–6x^2+0.002x+0.170	0.20	<0.001
Extensibility	y=–7.291E–6x^2+0.002x+0.331	0.10	<0.001
Strength	y=–131.278x^2+29212.353x+1.692E6	0.13	0.015
Toughness	y=–31.500x^2+7235.183x+2.922E5	0.14	0.003
Stiffness E_{max}	y=–523.168x^2+1.099E5x+1.490E7	0.05	0.359

n=254.

Journal of Experimental Biology (2017) 220, 2108-2119 doi:10.1242/jeb.145706

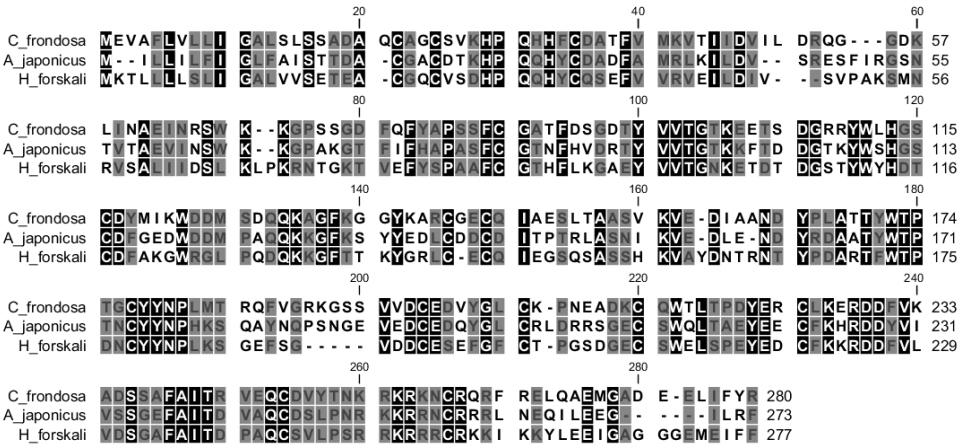

Fig. 6. Alignment of tensilin sequences from *Cucumaria frondosa* and *Apostichopus japonicus* with that from the Cuvierian tubules of *H. forskali*. The sequences were aligned with the software CLC. The shading represents the conserved amino acids (black: identical amino acid at the same position in the three sequences, grey: identical amino acid at the same position in two of the three sequences, white: different amino acids at the same position for the three sequences).

of proteins extracted from whole tubules as well as in immunohistochemistry on tubule sections. In western blots, strong labelling was observed for a protein band with an apparent molecular mass corresponding to Cuvierian tubule tensilin (i.e. 29 kDa; Fig. 8A). Two other bands, more weakly labelled, were also detected at an apparent molecular mass of 17 and 22 kDa (see also Appendix). In immunohistochemistry on tubule sections, a strong specific labelling was observed only at the level of the connective tissue layer (Fig. 8B–F). The labelling of the spherulocytes close to the inner epithelium was apparently non-specific as it was also observed in the negative controls (Fig. 8C). Extensive immunoreactivity of elongated cells running between the collagen fibres was apparent at higher magnification (Fig. 8D,E). The labelling took the form of spherical structures, about 0.5 µm in diameter, contained in these elongated cell processes, as shown by immunofluorescence (Fig. 8F).

DISCUSSION

Sea cucumbers are animals one could consider as vulnerable to predation because of their soft body wall and slow movements. Yet, they possess several defence systems including evisceration, the production of saponins (deterrent secondary metabolites) and, in some species, the ejection of Cuvierian tubules (Lawrence, 1987). These tubules work as a remarkable defence system by forming a sticky network to immobilise predators (Becker and Flammang, 2010). Their efficiency results from two major characteristics: their adhesivity and their capacity to resist traction forces. In addition, as Cuvierian tubules elongate up to 20 times their original length upon discharge, their mechanical design must reconcile an initial relative compliance to allow elongation with a later stiffening to resist traction. This paradox was investigated by measuring and comparing the mechanical properties of both quiescent (before elongation) and elongated Cuvierian tubules.

Tensile tests were first performed on quiescent Cuvierian tubules to investigate their response to elongation, even though this type of testing does not reflect exactly the natural process in which seawater is forcefully injected into the tubule lumen. The shape of the force–extension curves is characteristic: the force increases initially to reach a plateau of low force value, which persists for much of the extension and ends in a high peak before the tubule breaks. The

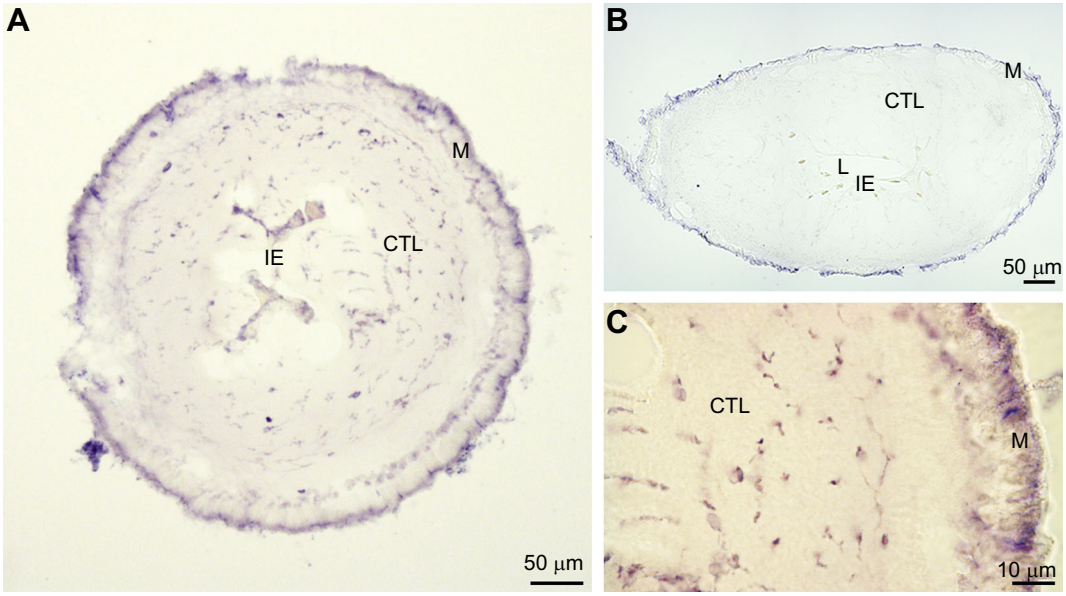

Fig. 7. Tensilin localisation in the quiescent Cuvierian tubules of *H. forskali* by *in situ* hybridisation. (A,B) Localisation of the tensilin mRNA on tubule transverse sections with antisense and sense (negative control) probes, respectively. (C) Tubule transverse section showing strongly labelled cell bodies scattered all over the connective tissue layer. CTL, connective tissue layer; IE, inner epithelium; L, lumen; M, mesothelium.

Journal of Experimental Biology (2017) 220, 2108-2119 doi:10.1242/jeb.145706

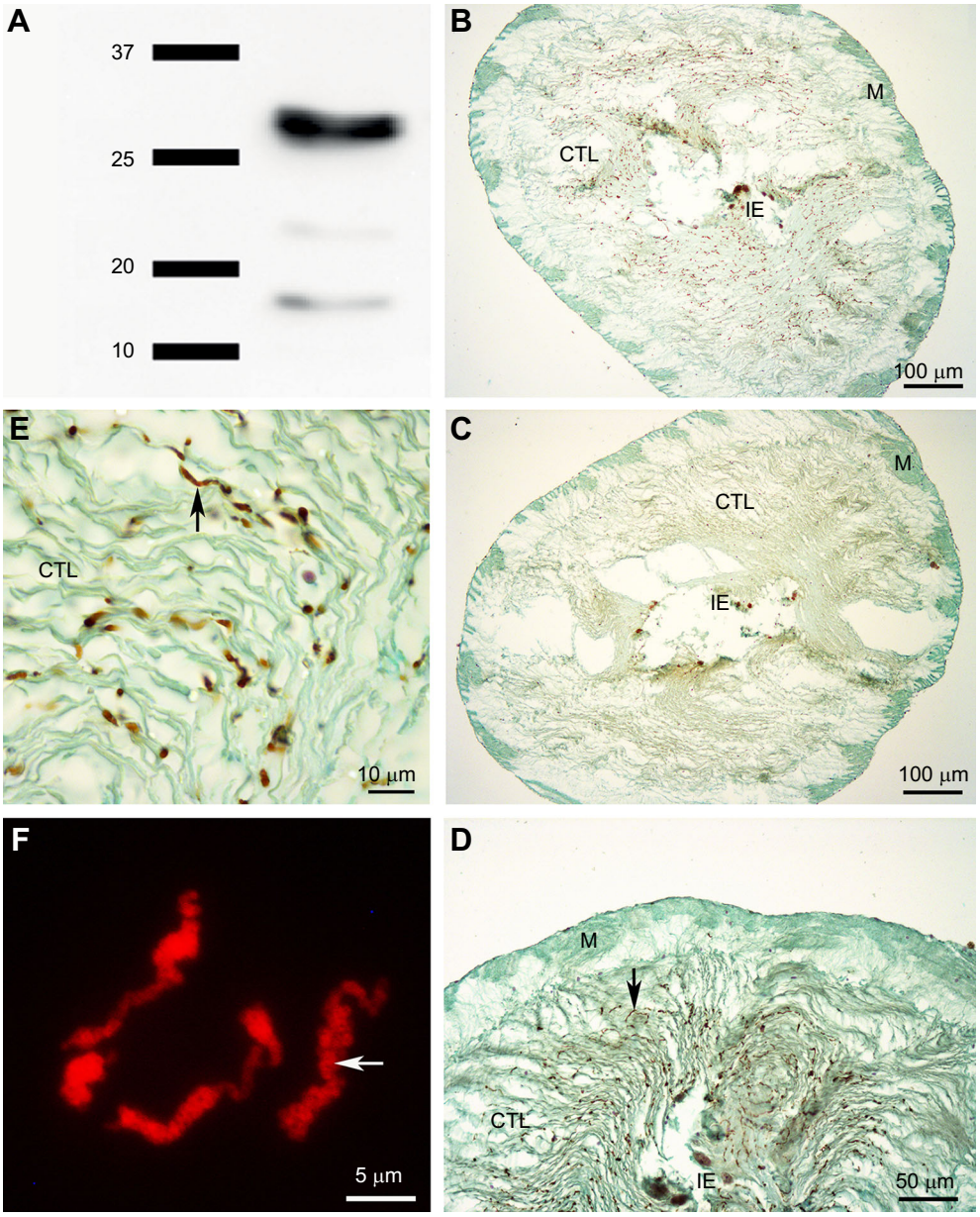

Fig. 8. Tensilin immunoreactivity. Western blot analysis (A) and immunohistochemical localisation (B–F) of tensilin in the Cuvierian tubules of *H. forskali*. (A) Western blot of proteins extracted from whole tubules immunolabelled with polyclonal antibody against the peptide VVTGNKETDTDGSTY (see Materials and methods). The most intensely stained band at about 29 kDa corresponds to the calculated molecular mass of tensilin. Molecular mass markers (kDa) are indicated on the left. (B,D) Quiescent tubule transverse sections labelled with the same antibody (immunoreactive cells are labelled in brown). Only cells distributed within the connective tissue layer are immunoreactive, the labelling of spherulocytes in the inner epithelium being non-specific. (C) Control section labelled with the pre-immune serum. (E,F) At higher magnification, elongated cell processes (arrows) are clearly visible with both immunoenzymatic and immunofluorescence methods, respectively. CTL, connective tissue layer; IE, inner epithelium; L, lumen; M, mesothelium.

corresponding stress–strain curve presents the same aspect except that the stress of the plateau increases slightly with strain because true stress was used in the calculation. Among biomaterials, curves of a similar shape are obtained for tensile tests performed on wool fibres (Vincent, 1990). The keratin that comprises wool consists mainly of α-helices stabilised by H-bonds. The first part of the stress–strain curve, presenting a high stiffness, reflects rupture of the H-bonds. Then, the α-helixes start to unravel and the stress remains relatively constant. At higher strain, it rises again quickly when the pull is exerted directly on the unravelled polypeptide chains (Vincent, 1990). Although Cuvierian tubules are more complex organs, their mechanical behaviour can be compared with the wool model because their connective tissue core comprises a large amount of collagen fibres laid out in several helices running parallel to the tubular long axis (VandenSpiegel and Jangoux, 1987). In the case of quiescent tubules, the surface area below the force–extension curve at the level of the plateau represents the energy necessary to stretch the helicoidally arranged collagen fibres. To facilitate tubule elongation, the force (and consequently the stress) at plateau therefore needs to be low. The Young's modulus (initial stiffness) could correspond to the stiffness of the matrix surrounding collagen fibres, including interactions between fibrils. Its value (0.04 MPa) is similar to that of soft connective tissues such as the sea anemone mesoglea (Vogel, 2013). At the end of the plateau, when the helices are unfolded, the peak force corresponds to the resistance of the extended collagen fibres to traction. However, although the beginning of the curves is reproducible among the different experiments, the end is much more variable and difficult to interpret.

The stress–strain curves of elongated tubules are completely different and more reminiscent, at least in their first part, of those of collagenous biomaterials (e.g. tendons). Indeed, these biomaterials usually present a J-shaped stress–strain curve in which the stress, initially low, increases exponentially until the material breaks (Vincent, 1990; Vogel, 2013). The first half of the stress–strain curve of the elongated Cuvierian tubules corresponds perfectly to a typical curve for a collagenous material. However, instead of a sudden rupture at the maximum stress, Cuvierian tubules undergo a

Journal of Experimental Biology

Journal of Experimental Biology (2017) 220, 2108-2119 doi:10.1242/jeb.145706

regular decrease of stress, by successive steps. The connective tissue layer of the tubule thus does not seem to behave as a single structure but as a set of substructures which break one after the other. These substructures presumably correspond to the collagen fibres which are arranged in interlocked helices (VandenSpiegel and Jangoux, 1987). Our observations also corroborate the assumption of Bailey et al. (1982) according to which, in Cuvierian tubules, the covalent bonds between collagen fibrils are always longitudinal, connecting them end-to-end, and not lateral. This arrangement of the covalent cross-links would allow sliding between the individual fibrils and/or fibres and, therefore, a high extensibility. Compared with a sudden break, the progressive breaking of a Cuvierian tubule almost doubles the area under the stress–strain curve and, consequently, doubles the tubule toughness. At equal strength, a predator will have to provide about twice as much energy to break a 'normal' Cuvierian tubule compared with a similar structure which would break abruptly. The values of strength, extensibility and stiffness for elongated tubules approach those of other collagen-based pliant composites such as mesoglea, skin or arterial wall (Wainwright, 1982; Vogel, 2013). These values are also close to those of sea star and sea urchin tube feet, which, like the tubules, contain a large amount of collagen (see Santos et al., 2009, for review). The much lower values of strength and stiffness for elongated Cuvierian tubules compared with those of tendons could be explained by the absence of transverse cross-links between the collagen fibres. Indeed, there is a direct relationship between the quantity of these cross-links and the mechanical properties of collagenous material (Bailey et al., 1982). These lower values, however, are partially compensated for by the breaking mode of the tubules, as explained above, which leads to a tubule toughness only slightly lower than the toughness of tendons (Vogel, 2013). In addition, when Cuvierian tubules are subjected to a higher speed of traction, the values of extensibility, strength and toughness increase. From the animal's point of view, this positive strain rate dependence would be beneficial, its Cuvierian tubules being tougher if the predator pulls on them faster. A similar strain rate dependence has been reported by Zahn et al. (1973), although in their study, extensibility and strength were not affected similarly.

Our results on the mechanical properties of Cuvierian tubules reconcile the only two previous studies on tubule biomechanics, which had apparently diverging conclusions (Zahn et al., 1973; Bailey et al., 1982). Although their text was misleading, Bailey et al. (1982) clearly worked on quiescent tubules. The stress–strain curve they show (fig. 2 in their article) indeed coincides with the first part (plateau) of our curves, their plateau extending from strain 1.5 to 14 (nominal values) for a nominal stress of 50 Pa. Their curve, however, did not reach the final stress peak, which also occurred in some of our experiments. In contrast, the stress–strain curve presented by Zahn et al. (1973) corresponds perfectly to the curves we obtained for elongated tubules, the values of strength they measured (6000 kPa) being similar to our measurements (approximately 3300 kPa). The two studies are thus not contradictory, they just tested different types of Cuvierian tubules: quiescent for Bailey et al. (1982) versus elongated for Zahn et al. (1973).

Morphological observations indicate that, during Cuvierian tubule elongation, the lumen diameter increases whereas the thickness of the connective tissue layer decreases because the helicoidally arranged collagen fibres stretch (see also VandenSpiegel and Jangoux, 1987). Within the connective tissue layer, several cell types appear severely modified or even disappear during tubule elongation: the two types of neurosecretory-like cells, the vacuolar cells and the spherulocytes. Among these cells, neurosecretory-like cells particularly caught our interest because they are morphologically similar to the juxtaligamental cells found in echinoderm MCTs and characterised by processes containing electron-dense granules (Wilkie, 1996, 2005). This is a first argument in favour of the occurrence of a MCT in Cuvierian tubules because all MCTs described to date contain juxtaligamental cells, whereas the few definitely non-mutable collagenous structures examined lack these cells (Wilkie, 2002; Wilkie et al., 2003). Two types of juxtaligamental cells generally co-occur in a same MCT, being distinguishable by the size and shape of their granules (Wilkie, 1996; Koob et al., 1999). In Cuvierian tubules, only type 1 neurosecretory-like cells, the type enclosing large secretory granules, were always closely associated with collagen fibrils. It can be assumed therefore that these cells are juxtaligamental cells, characteristic of a new type of MCT.

Although morphology suggests the presence of a MCT in Cuvierian tubules, only mechanical testing and molecular characterisation can demonstrate this presence unequivocally. Mechanical measurements were performed on both quiescent and elongated tubules after incubation in seawater containing Triton X-100, a cell-lysing treatment known to expose the connective tissue to the contents of disrupted cells, thus influencing its physiological state and mechanical properties. When exposed to this solution, there was an increase in the initial stiffness and force at plateau for quiescent tubules, and an increase in stiffness and toughness for elongated tubules. Cell disruption therefore induces a stiffening response in the two types of tubule, as previously observed in most other echinoderm MCTs. Tensilin is one of the proteins responsible for MCT stiffening and was reported to be present in juxtaligamental cells in the dermis of *C. frondosa* (Tipper et al., 2003; Wilkie, 2005). In Cuvierian tubules, tensilin and its coding mRNA were detected in the connective tissue layer, more precisely at the level of the neurosecretory-like cells. Our study is the first to use *in situ* hybridisation and immunohistochemistry to analyse the expression of tensilin in MCT, except for the study of Tipper et al. (2003), which reported (but did not illustrate) the immunolabelling of juxtaligamental cells using anti-tensilin antibodies. Based on the shape, size and location of labelled cells, both the *in situ* hybridisation and immunohistochemistry experiments indicate that type 1 neurosecretory-like cells would be the juxtaligamental cells of Cuvierian tubules. In addition, the size of their immunoreactive intracytoplasmic structures corresponds to the size of type 1 neurosecretory-like cell granules. However, only immunogold labelling of TEM sections could prove unambiguously that type 1 neurosecretory-like cells are the cells expressing tensilin. As previously described, the number of granules in type 1 neurosecretory-like cell processes decreases during elongation. Tensilin could be released during this phenomenon and be responsible for the irreversible stiffening occurring in Cuvierian tubules. The fact that the cell-lysing solution can still affect tubule stiffness after elongation could then be due to the presence of the remaining cells releasing their contents. In *C. frondosa*, it has been proposed that one type of granule would enclose a stiffener (tensilin) and the other a plasticiser (Koob et al., 1999). In the particular case of Cuvierian tubules, no plasticiser is needed as they are single-use organs. The second type of granule could therefore contain another stiffening factor as described in the dermis of *Holothuria leucospilota* (Tamori et al., 2006; Yamada et al., 2010) or, more likely, belong to a nerve cell and have a control function.

In the dermis of *C. frondosa*, a third cell type with large granules apparently acts as an important regulator of tissue stiffness (Koob et al., 1999). This cell shares some resemblance with the

Journal of Experimental Biology (2017) 220, 2108-2119 doi:10.1242/jeb.145706

spherulocytes of Cuvierian tubules. Based on TEM observations, VandenSpiegel and Jangoux (1987) showed that, when Cuvierian tubules elongate, their inner epithelium is torn apart and the contents of the spherulocytes are released towards the tubule lumen. These authors suggested that spherule constituents could form a cement layer at this level, improving the rigidity of elongated tubules. Alternatively, the spherule contents, which might include enzymes (Flammang et al., 2002), could diffuse into the connective tissue layer, where they could induce intermolecular cross-link formation with the same final effect of increasing tubule rigidity. In our measurements, however, all parameters except stiffness evolved during the time elapsed after tubule expulsion, first increasing until they reached a maximum after 2 h and then decreasing. As for vacuolar cells, they would be involved in saponin production (see Van Dyck et al., 2010).

Holothuroid Cuvierian tubules present a very effective mechanical design. Indeed, they are faced with the need to be highly compliant to be expelled and to elongate and then to be as strong as possible in order to resist the tractions of predators. It is their remarkable structural organisation, with a helical arrangement of long, individual collagen fibres, together with the presence of a MCT and, possibly, of another stiffening process which enables this adaptability and transition from a 'soft' to a 'stiff' state. Cuvierian tubules appear to enclose a new type of MCT which shows irreversible stiffening, as opposed to the three other types of MCT described to date, which can undergo reversible stiffening and destiffening, with the possibility of irreversible destabilisation (associated with autotomy), or irreversible destabilisation only (again, associated with autotomy) (Wilkie, 1996).

APPENDIX

Transcriptome sequencing and *de novo* assembly

RNA extraction, library construction and sequencing were performed at the GIGA Genomics platform (Liège, Belgium). After dissection, quiescent tubules were immediately frozen with liquid nitrogen and stored at −80°C until use. Total RNA was extracted from these tubules using Trizol (Life Technologies, Carlsbad, CA, USA) and its quality was assessed using a Bioanalyser 2100 (Agilent, Santa Clara, CA, USA). Truseq Stranded mRNA Sample Preparation kit (San Diego, CA, USA) was used to prepare a library from 500 ng of total RNA. Poly-adenylated RNAs were purified with oligo (dT)-coated magnetic beads [Sera-Mag Magnetic Oligo(dT) beads, Illumina, San Diego, CA, USA] and then chemically fragmented to a length of 100–400 nucleotides – with the majority of the fragments at about 200 bp – by using divalent cations at 94°C for 5 min. These short fragments were used as a template for reverse transcription using random hexamers to synthesise cDNA, followed by end reparation and adaptor ligation according to the Illumina protocol. Finally, the ligated library fragments were purified and enriched by solid-phase PCR following the Illumina protocol. The library quality was validated using the Bioanalyser 2100. The high-throughput sequencing was conducted with a HiSeq 2000 platform (Illumina) to obtain 2×100 bp paired-end reads according to the manufacturer's instructions. Real-time quality control was performed to ensure that most read quality scores were higher than 30.

Transcriptome quality was checked using Fast QC software (Babraham Bioinformatics, Cambridge, UK). The Trinity software suite (Grabherr et al., 2011), which comprises a quality filtering function, was used with default parameters to *de novo* assemble the raw reads with overlapping nucleic acid sequences into contigs and unigenes (clusters of contigs).

Cuvierian tubule transcriptome sequencing generated 179,601,824 raw reads with a length of 100 bp; these have been deposited in the GenBank sequence read archive (SRA) under accession number SRP095088. The GC percentage reached 40% while the *N* percentage value was 0. The average quality per reads was 38. After *de novo* assembly using Trinity software, 156,918 transcripts were obtained with a mean length of 914 bp and a N_{50} (median length) of 466 bp. The size of the transcripts ranged from 201 to 17,237 bp. Transcripts were further clustered into 98,969 non-redundant sequences (i.e. unigenes) with a mean length of 649 bp and a N_{50} of 359 bp. The statistics for the sequencing output data and assembly results are summarised in Table S1.

The distribution of the length of transcripts after assembly is presented in Fig. S1. It shows a decreasing number of transcripts with longer sequences. A high percentage of short transcripts (>299 bp) is present but seems unavoidable, as it is the case for other transcriptome assemblies too (Du et al., 2012; Delroisse et al., 2015). The graph representing the length distribution of unigenes presents the same pattern (not shown).

Tensilin expression in Cuvierian tubules

Evidence at the mRNA level

The Cuvierian tubule transcriptome of *H. forskali* was used to search for tensilin mRNAs using a tBLASTn approach and the protein sequences of *C. frondosa* and *S. japonicus* (NCBI accession number AAK61535 and KR002726.1, respectively) as queries. Seventeen transcripts were retrieved with a bit score above 80 (Table S2). Among them, the 12 transcripts named comp85694 varied only in the 5′ UTR and not in the ORF. They were therefore considered as coding for a same protein. After *in silico* translation (Expasy, Translate tool), the six protein sequences were aligned (Fig. S2).

Evidence at the protein level

Among the six transcripts whose translated sequences presented a significant homology with known tensilins, we selected transcript comp85694 for further investigation because it was the most abundant (in terms of FPKM) in the transcriptome and because we identified peptide sequences specific of this transcript at the proteomic level (Fig. S3) (Demeuldre, 2015). The full-length protein sequence comprises a 20 amino acid-long putative signal peptide followed by a proprotein sequence of 257 amino acids with a calculated molecular mass of 29 kDa (Expasy, ProtParam tool) (Fig. S3).

To further confirm the presence of tensilin in the Cuvierian tubules, we raised polyclonal antibodies directed against one peptide selected in the translated sequence of comp85694 (Fig. S3). These antibodies were used in western blots of proteins extracted from whole tubules and labelled a protein band with an apparent molecular mass corresponding to Cuvierian tubule tensilin (i.e. 29 kDa) (Fig. S4).

Acknowledgments

We would like to thank Prof. Denis Nonclerq and Mrs Françoise Coulon for the use of the cryostat. This study is a contribution of the Centre Interuniversitaire de Biologie Marine (CIBIM).

Competing interests

The authors declare no competing or financial interests.

Author contributions

Conceptualization: E.H., P.F.; Methodology: M.D., E.H., M.B., B.L., S.V.D.; Formal analysis: E.H., P.L.; Investigation: M.D., E.H., M.B., S.V.D., P.F.; Resources: B.L., R.W.; Data curation: P.L.; Writing - original draft: M.D., E.H., M.B., B.L., S.V.D., R.W.,

P.L., P.F.; Writing - review & editing: E.H., M.B., B.L., R.W., P.L., P.F.; Visualization: M.D., E.H., M.B., B.L.; Supervision: E.H., P.F.; Project administration: P.F.; Funding acquisition: P.F.

Funding
This work was supported partially by the US Office of Naval Research (grant no. N00014-99-1-0853) and by COST Action TD0906. M.D. and S.V.D. benefited from a FRIA doctoral grant (Fonds De La Recherche Scientifique - FNRS) (Belgium). P.F. is Research Director of the Fund for Scientific Research of Belgium (Fonds De La Recherche Scientifique - FNRS). B.L. was a recipient of a DOC Fellowship of the Austrian Academy of Sciences at the Institute of Zoology, University of Innsbruck, and is supported by a PhD Fellowship of the University of Innsbruck. PL is supported by Austrian Science Fund (FWF): [P 25404-B25].

Data availability
The raw reads and the tensilin sequence from the Cuvierian tubules of *H. forskali* have been deposited in GenBank (accession number SRP095088 and KY609179.1, respectively).

Supplementary information
Supplementary information available online at
http://jcs.biologists.org/lookup/doi/10.1242/jeb.145706.supplemental

References
Bailey, A. J., Gathercole, L. J., Dlugosz, J., Keller, A. and Voyle, C. A. (1982). Proposed resolution of the paradox of extensive crosslinking and low tensile strength of Cuvierian tubule collagen from the sea cucumber *Holothuria forskali*. *Int. J. Biol. Macromol.* **4**, 329-334.
Barbaglio, A., Tricarico, S., Ribeiro, A., Ribeiro, C., Sugni, M., Di Benedetto, C., Wilkie, I., Barbosa, M., Bonasoro, F. and Candia Carnevali, M. D. (2012). The mechanically adaptive connective tissue of echinoderms: Its potential for bio-innovation in applied technology and ecology. *Mar. Environ. Res.* **76**, 108-113.
Becker, P. and Flammang, P. (2010). Unravelling the sticky threads of sea cucumbers – a comparative study on cuvierian tubule morphology and histochemistry. In *Biological Adhesive System - From Nature to Technical and Medical Applications* (ed. J. von Byern and I. Grunwald), pp. 87-98. Wien: Springer.
Delroisse, J., Ortega-Martinez, O., Dupont, S., Mallefet, J. and Flammang, P (2015). De novo transcriptome of the European brittle star *Amphiura filiformis* pluteus larvae. *Mar. Genomics* **23**, 109-121.
Demeuldre, M. (2015). Defence mechanisms is sea cucumbers: Morphology, biochemistry and mechanics of Cuvierian tubules in two species from the genus *Holothuria*. *PhD Thesis*, University of Mons.
Demeuldre, M., Ngo, T. C., Hennebert, E., Wattiez, R., Leclère, P. and Flammang, P. (2014). Instantaneous adhesion of Cuvierian tubules in the sea cucumber. *Biointerphases* **9**, 029016.
Du, H., Bao, Z., Hou, R., Wang, S., Su, H., Yan, J., Tian M., Li Y., Wei W., Lu W., Hu X., Wang S. and Hu, J (2012). Transcriptome sequencing and characterization for the sea cucumber *Apostichopus japonicus* (Selenka, 1867). *PLoS One* **7**, e33311.
Flammang, P., Ribesse, J. and Jangoux, M. (2002). Biomechanics of adhesion in sea cucumber Cuvierian tubules (Echinodermata, Holothuroidea). *Integr. Comp. Biol.* **42**, 1107-1115.
Flammang, P., Santos, R. and Haesaerts, D. (2005). Echinoderm adhesive secretions: from experimental characterization to biotechnological applications. In *Marine Molecular Biotechnology: Echinodermata* (ed. V. Matranga), pp. 201-220. Berlin: Springer-Verlag.
Flammang, P., Demeuldre, M., Hennebert, E. and Santos, R. (2016). Adhesive secretions in echinoderms: a review. In *Biological Adhesives*, 2nd edn. (ed. A. M. Smith), pp. 193-222. Cham: Springer International Publishing.
Gabe, M. (1968). *Techniques Histologiques*. Paris: Masson.
Grabherr, M. G., Haas, B. J., Yassour, M., Levin, J. Z., Thompson, D. A., Amit, I., Adiconis, X., Fan, L., Raychowdhury, R., Zeng, Q. et al (2011). Full-length transcriptome assembly from RNA-Seq data without a reference genome. *Nature Biotechnol.* **29**, 644-652.
Haas, B. J., Papanicolaou, A., Yassour, M., Grabherr, M., Blood, P. D., Bowden, Couger, M. B., Eccles, D., Li, B., Lieber, M. et al. (2013). De novo transcript sequence reconstruction from RNA-seq using the Trinity platform for reference generation and analysis. *Nature Protoc.* **8**, 1494-1512.
Hamel, J. F. and Mercier, A. (2000). Cuvierian tubules in tropical holothurians: usefulness and efficiency as a defence mechanism. *Mar. Freshw. Behav. Phy.* **33**, 115-139.
Koob, T., Koob-Emunds, M. and Trotter, J. (1999). Cell-derived stiffening and plasticizing factors in sea cucumber (*Cucumaria frondosa*) dermis. *J. Exp. Biol.* **202**, 2291-2301.
Lawrence, J. M. (1987). *A Functional Biology of Echinoderms*. London: Croom Helm.
Lengerer, B., Pjeta, R., Wunderer, J., Rodrigues, M., Arbore, R., Schärer, L., Berezikov, E., Hess, M. W., Pfaller, K., Egger, B. et al. (2014). Biological adhesion of the flatworm *Macrostomum lignano* relies on a duo-gland system and is mediated by a cell type-specific intermediate filament protein. *Front. Zool.* **11**, 12.
Mo, J., Prévost, S. F., Blowes, L. M., Egertová, M., Terrill, N. J., Wang, W., Elphick, M. R. and Gupta, H. S. (2016). Interfibrillar stiffening of echinoderm mutable collagenous tissue demonstrated at the nanoscale. *Proc. Natl. Acad. Sci. USA* **113**, E6362-E6371.
Müller, M. E. G., Zahn, R. K. and Schmid, K. (1972). The adhesive behaviour in Cuvierian tubules of *Holothuria forskali* biochemical and biophysical investigations. *Cytobiologie* **5**, 335-351.
Peng, Y. Y., Glattauer, V., Skewes, T. D., White, J. F., Nairn, K. M., McDevitt, A. N., Elvin, C. M., Werkmeister, J. A., Graham, L. D. and Ramshaw, J. A. M. (2011). Biomimetic materials as potential medical adhesives –composition and adhesive properties of the material coating the Cuvierian tubules expelled by *Holothuria dofleinii*. In *Biomaterials- Physics and Chemistry* (ed. R. Pignatello), pp. 245-258. Rijeka: InTech Press.
Santos, R., Hennebert, E., Varela Coelho, A. and Flammang, P. (2009). The echinoderm tube foot and its role in temporary underwater adhesion. In *Functional Surfaces in Biology*, Vol. 2 (ed. S. Gorb), pp. 9-42. Heidelberg: Springer.
Shadwick, R. E. (1992). Soft composites. In *Biomechanics-Materials. A Practical Approach* (ed. J. F. V. Vincent), pp. 133-164. Oxford, UK: Oxford University Press.
Tamori, M., Yamada, A., Nishida, N., Motobayashi, Y., Oiwa, K. and Motokawa, T. (2006). Tensilin-like stiffening protein from *Holothuria leucospilota* does not induce the stiffest state of catch connective tissue. *J. Exp. Biol.* **209**, 1594-1602.
Tipper, J. P., Lyons-Levy, G., Atkinson, M. A. and Trotter, J. A. (2003). Purification, characterization and cloning of tensilin, the collagen-fibril binding and tissue-stiffening factor from *Cucumaria frondosa* dermis. *Matrix Biol.* **21**, 625-635.
Trotter, J. A., Tipper, J., Lyons-Levy, G., Chino, K., Heuer, A. H., Liu, Z., Mrksich, M., Hodneland, C., Dillmore, W. S., Koob, T. J. et al. (2000). Towards a fibrous composite with dynamically controlled stiffness. Lessons from echinoderms. *Biochem. Soc. Trans.* **28**, 357-362.
Van Dyck, S., Flammang, P., Meriaux, C., Bonnel, D., Salzet, M., Fournier, I. and Wisztorski, M. (2010). Localization of secondary metabolites in marine invertebrates: contribution of MALDI MSI for the study of saponins in cuvierian tubules of *H. Forskali*. *PLoS ONE* **5**, e13923.
VandenSpiegel, D. and Jangoux, M. (1987). Cuvieran tubules of the holothuroid *Holothuria forskali* (Echinodermata): a morphofunctional study. *Mar. Biol.* **96**, 263-275.
VandenSpiegel, D., Jangoux, M. and Flammang, P. (2000). Maintaining the line of defense: regeneration of cuvierian tubules in the sea cucumber *Holothuria forskali* (Echinodermata, Holothuroidea). *Biol. Bull.* **198**, 34-49.
Vincent, J. F. V. (1990). *Structural Biomaterials*. New Jersey : Princeton University Press.
Vogel, S. (2013). *Comparative Biomechanics – Life's Physical World*, 2nd edn. Princeton: Princeton University Press.
Wainwright, S. A. (1982). *Mechanical Design in Organisms*. New Jersey: Princeton University Press.
Wilkie, I. C. (1996). Mutable collagenous tissues: extracellular matrix as mechano-effector. In *Echinoderm Studies* (ed. M. Jangoux and J. M. Lawrence), pp. 61-102. Rotterdam: Balkema.
Wilkie, I. C. (2002). Is muscle involved in the mechanical adaptability of echinoderm mutable collagenous tissue? *J. Exp. Biol.* **205**, 159-165.
Wilkie, I. C. (2005). Mutable collagenous tissue: overview and biotechnological perspective. In *Marine molecular biotechnology: Echinodermata* (ed. V. Matranga), pp. 221-250. Berlin: Springer-Verlag.
Wilkie, I. C., Candia Carnevali, M. D. and Bonasoro, F. (2003). A non-mutable collagenous structure? Organisation and physiology of the compass-rotular ligament of the echinoid lantern. In *Echinoderm Research 2001* (ed. J.P. Féral and B. David), pp. 121-130. Lisse: Swets & Zeitlinger.
Yamada, A., Tamori, M., Iketani, T., Oiwa, K. and Motokawa, T. (2010). A novel stiffening factor inducing the stiffest state of holothurian catch connective tissue. *J. Exp. Biol.* **213**, 3416-3422.
Zahn, R. K., Müller, W. E. G. and Michaelis, M. (1973). Stiking mechanisms in adhesive organs from *Holothuria*. *Res. Mol. Biol.* **2**, 47-88.